APPLIED AND ENVIRONMENTAL MICROBIOLOGY, Nov. 1993, p. 3840–3849 Vol. 59, No. 11
0099-2240/93/113840-10$02.00/0

Distribution of Sulfate-Reducing Bacteria, O_2, and H_2S in Photosynthetic Biofilms Determined by Oligonucleotide Probes and Microelectrodes

NIELS BIRGER RAMSING,† * MICHAEL KÜHL,† AND BO BARKER JØRGENSEN†

Department of Microbial Ecology, Institute of Biological Sciences, University of Aarhus, Ny Munkegade, DK-8000 Aarhus C, Denmark

Received 28 April 1993/Accepted 28 July 1993

The vertical distribution of sulfate-reducing bacteria (SRB) in photosynthetic biofilms from the trickling filter of a sewage treatment plant was investigated with oligonucleotide probes binding to 16S rRNA. To demonstrate the effect of daylight and photosynthesis and thereby of increased oxygen penetration, we incubated two 4-mm-thick biofilm samples in darkness or exposed to light at natural intensity. Gradients of O_2, H_2S, and pH were examined with microelectrodes during incubation. The samples were subsequently frozen with liquid nitrogen and sliced on a cryomicrotome in 20-μm vertical slices. Fluorescent-dye-conjugated oligonucleotides were used as "phylogenetic" probes to identify single cells in the slices. Oligonucleotide sequences were selected which were complementary to short sequence elements (16 to 20 nucleotides) within the 16S rRNA of sulfate-reducing bacteria. The probes were labeled with fluorescein or rhodamine derivatives for subsequent visualization by epifluorescence microscopy. Five probes were synthesized for eukaryotes, eubacteria, SRB (including most species of the δ group of purple bacteria), *Desulfobacter* spp., and a nonhybridizing control. The SRB were unevenly distributed in the biofilm, being present in all states from single scattered cells to dense clusters of several thousand cells. To quantify the vertical distribution of SRB, we counted cells along vertical transects through the biofilm. This was done in a blind experiment to ascertain the reliability of the staining. A negative correlation between the vertical distribution of positively stained SRB cells and the measured O_2 profiles was found. The distribution differed in light- and dark-incubated samples presumably because of the different extensions of the oxic surface layer. In both cases the SRB were largely restricted to anoxic layers.

Photosynthetic biofilms from trickling filters have been used in several studies of microbial processes in environments with steep chemical gradients (e.g., of oxygen metabolism [16, 23], sulfur metabolism [25], and nitrogen metabolism [8]). They constitute a convenient experimental system, which in many respects is similar to aquatic sediments, microbial mats, or natural epiphytic and epilithic biofilms. Biofilms are compact microbial communities, stratified with morphologically distinctive layers, in which many different processes occur simultaneously in close proximity (24). The metabolic rates are extremely high and respond fast to changes in ambient light, oxygen, nutrient content of overlying water, etc. The predominant metabolic processes are stratified and subdivide the biofilm into functional layers.

Diurnal cycles of incident light—and consequently of photosynthetic activity—induce large fluctuations in oxygen concentrations within the biofilm (23, 25). The varying O_2 concentration and its influence on the depth distribution and activity of sulfate-reducing bacteria (SRB) are interesting in view of two recent accounts of sulfate reduction in the presence of oxygen (7, 14). Both studies deal with microbial mats from hypersaline environments; however, other investigators have made related observations in more widespread habitats (43, 44). Jørgensen and Bak investigated the distribution of SRB in near-shore marine sediments, Kattegat, Denmark (19). Using a most-probable-number approach with a selective medium for SRB, they found the highest density of SRB in the oxic zone just below the surface. These organisms apparently belong to a novel type of slow-growing, gas-vacuolated sulfate reducers (19). Anoxic microenvironments have previously been assumed to explain such a distribution (18, 48); however, the natural occurrence and importance of anoxic microenvironments in oxic sediments have never been directly demonstrated.

To investigate the distribution of sulfate-reducing bacteria in a complex stratified environment such as a biofilm, we used fluorescent oligonucleotide probes that bind to rRNA within these bacteria. The application of this technique in microbial ecology has recently been reviewed by Ward et al. (46, 47) and Stahl et al. (38, 40). Oligonucleotide probes have been used successfully in a variety of environments. In complex environments most applications have involved the characterization of immobilized nucleotides isolated from a sample by the quantitative binding of selected ^{32}P-labeled probes (34, 39). In simple environments, in situ hybridization with fluorescent probes has been used qualitatively (5, 6) to identify unculturable organisms (3, 37), to evaluate bacterial activity (30), to characterize isolates (22, 41), or to develop and extend the technique (4, 10, 15, 49). Two notable exceptions are (i) a quantitative study of the natural bacterioplankton by using fluorescent probes for the three kingdoms (17) and (ii) a recent quantitative study of activated sludge with probes for different groups of proteobacteria (45).

The oligonucleotide sequences of the probes used here were mostly devised by Amann et al. (4) to be complementary to short sequence elements (16 to 20 nucleotides) within the 16S rRNA. The eukaryotic probe was devised by Gio-

* Corresponding author.
† Present address: Max Planck Institute for Marine Microbiology, Fahrenheitstrasse 1, D-28359 Bremen 3, Germany.

vannoni et al. (15). These probe sequences have been used in other studies to identify individual cells in sulfidogenic biofilms, less than 10 μm thick, from anaerobic fixed-bed bioreactors (6) or to identify sulfate-reducing bacterial ectosymbionts on anaerobic ciliates (13).

In the present study we have investigated the distribution of SRB in a photosynthetic biofilm from a wastewater trickling filter. Incubations were made with and without light to investigate the effects of different oxygen penetrations on the vertical distribution of SRB. The distribution of probe-stained cells was estimated by counting positively stained cells in vertical transects across several biofilm slices. This was done in a blind experiment (in which some slices were stained with an SRB probe, some with a *Desulfobacter* probe, and some with a nonhybridizing control probe) to minimize subjectivity in the quantification process. In this study we thus present the first attempt to use in situ hybridization of phylogenetic oligonucleotide probes to quantify the occurrence of a specific bacterial group in a dense microbial community. A combined study of the chemical and optical gradients in, and the observed microstructure of, such a biofilm are presented elsewhere (32).

(A preliminary account of part of this work appeared in *Proceedings of the 6th International Symposium on Microbial Ecology.*)

MATERIALS AND METHODS

Biofilm samples. The biofilm grew on stones from the light-exposed surface of a trickling filter at a municipal wastewater treatment plant in Skødstrup, Denmark (32). The stones in the filter were drenched with raw sewage from a settling tank every 20 s. The sewage contained 0.5 to 1.0 mM sulfate. The biofilm was ca. 5 mm thick with a uniform dark green appearance and a photosynthetic community dominated by filamentous cyanobacteria (*Oscillatoria* spp.) (16, 24, 32). Stones with a homogeneous biofilm cover were collected from the trickling filter, and their sides and bottoms were cleaned to remove most of the motile population of sludgeworms (*Tubifex* spp.). Two smooth areas of the biofilm, 30 by 30 mm, ca. 5 mm thick, were selected and transferred to solidifying (30°C) 1% agar plates. Agar was applied around the edges of the sample to attach it, and the agar plates were submerged in aerated tap water with the addition of 0.5 mM Na_2SO_4, 0.1 mM sodium acetate, and 0.1 mM sodium lactate. Both plates were incubated for 48 h at 20°C. One plate was permanently illuminated with cold light from a halogen lamp at a light intensity of 35 μmol of photons m^{-2} s^{-1}. The other plate was incubated in darkness.

Microelectrodes. During and after incubation, we measured oxygen, pH, and sulfide profiles with microelectrodes as described previously (16, 25, 32). Oxygen was measured with a Clark type O_2 microelectrode connected to a picoamperemeter and a strip chart recorder (35). Photosynthetic rates were measured as the initial rate of oxygen depletion after a brief (<4-s) eclipse of the light source (36). Oxygen profiles were measured throughout the 48-h incubation period, whereas photosynthesis, pH, and sulfide measurements were made only at the end of incubation.

Cutting of biofilm samples. Immediately after the last microelectrode measurements, a small cube of each biofilm sample was removed (ca. 5 by 5 by 5 mm). The biofilm samples were placed on filter paper, embedded in OCT compound (Tissue-Tek II; Miles, Elkhart, Ind.), and frozen within 10 to 20 s by positioning the samples above a small container with evaporating liquid N_2. The freezing procedure was as rapid as possible to avoid migration of organisms. The frozen samples were cut into 20-μm-thick vertical slices with a cryomicrotome at −21°C. The slices were placed on gelatin-coated slides, which improved adhesion during the subsequent fixation, dehydration, and hybridization procedures.

Reference cells. Three different mixtures of known reference cells (1 μl each) were deposited next to the biofilm slice to serve as internal controls of hybridization efficiency. The first cell mixture contained the following species from pure cultures: *Escherichia coli* (donated by B. Hestbech, Institute of Medical Microbiology, University of Aarhus, Aarhus, Denmark), *Saccharomyces cervisiae* (donated by D. Schmidt, MPI for Biophysical Chemistry, Göttingen, Germany), and *Desulfovibrio vulgaris* DSM1744. The second contained *Pseudomonas cepacia*, *Pseudomonas aeroginosa*, and *Desulfobulbus propionicus*. The third contained *Pseudomonas fluorescens*, *Desulfovibrio gigas* DSM1389, and *Desulfobacter curvatus*. The three *Pseudomonas* species were donated by J. Sørensen, Royal Veterinary and Agricultural University, Copenhagen, Denmark; the two *Desulfovibrio* species were donated by R. Lillebæk, MPI for Marine Microbiology, Bremen, Germany; and the other SRB were donated by M. F. Isaksen, Institute of Biology, University of Aarhus. All reference cells were harvested in log phase, washed in phosphate-buffered saline (PBS), fixed in a fresh preparation of 4% paraformaldehyde in PBS for 1 to 2 h at room temperature, and stored at −25°C in a 1:1 mixture of pure ethanol and PBS.

Fixation and prehybridization. The biofilm slices were fixed with paraformaldehyde (4% in PBS) at room temperature for up to 1 h. After air drying, the cells were postfixed and dehydrated with 50, 80, and 100% ethanol. The dry slides were subsequently submerged in a $NaBH_4$ solution (50 mM in 100 mM Tris-HCl [pH 8]) and left for 30 min in the dark, then briefly rinsed with distilled water and treated for 5 min with 0.2 M HCl in 0.1% Triton X-100. The ethanol dehydration substantially reduced the inherent fluorescence in the biofilm slices. It also increased probe penetration through bacterial cell walls. The $NaBH_4$ treatment and the HCl treatment reduced the inherent fluorescence but had no effect on the hybridization efficiency. The slices were finally rinsed in distilled water and submerged for at least 10 min in a prehybridization solution consisting of 21% formamide in 5× SSC (1× SSC is 0.15 M NaCl plus 0.015 M sodium citrate). The slides could be stored for a few days at −25°C without substantial loss of hybridization efficiency.

Design of oligonucleotide probes. The probes were designed by other investigators (see below) with a data base of about 250 complete and partial 16S rRNA sequences. Four different probes were used (all numbering lists the corresponding positions in *Escherichia coli* 16S rRNA). They included (i) a general probe for eukaryotes (5′-GGG CAT CAC AGA CCT G-3′; positions 1209 to 1224), (ii) a probe for all eubacteria (5′-GCT GCC TCC CGT AGG AGT-3′; positions 338 to 355), (iii) a general probe for SRB (5′-CGG CGT CGC TGC GTC AGG-3′; positions 385 to 402), (iv) a probe specific for the genus *Desulfobacter* [5′-T(C/A)C GCA (G/A)AC TCA TCC CCA AA-3′; positions 502 to 516], and (v) a negative control probe (5′-CCT GAC GCA GCG ACG CCG-3′), which is complementary to the probe for SRB and which should be incapable of hybridizing with rRNA.

The general probe for SRB has been shown to label species in the δ-group of purple bacteria including the genera *Desulfovibrio*, *Desulfobacterium*, *Desulfobulbus*, *Desulfosarcina*, *Desulfococcus*, *Desulfomonas*, *Desulfobacter*, and

Myxococcus (4). The hybridization affinities for species in the last two genera are reduced due to a single-base-pair mismatch within the sequence. SRB of the genus *Desulfotomaculum* do not belong to the δ-group of purple bacteria and are thus not stained (11). The probe sequences were all taken from Amann et al. (4), except for the eukaryotic probe sequence which was published by Giovannoni et al. (15). The nonhybridizing control probe was a gift from R. Amann, Technische Universität, Munich, Germany.

Oligonucleotide synthesis, labeling, and purification. The oligodeoxynucleotides were synthesized by conventional phosphoramidite chemistry with an automated synthesizer as described previously (31). A primary amino group on a hexyl-phosphate linker was introduced at the 5′ end of the oligonucleotides by an extra cycle of phosphoramidite synthesis with Aminolink-2 [6-(4-monomethoxytritylamino) hexyl - (2 - cyanoethyl)(*N*,*N* - diisopropyl) - phosphoramidite (Applied Biosystems)]. Spin-down gel-filtration with Sephadex G-25 F columns (Pharmacia, Uppsala, Sweden) was used to remove protection groups prior to labeling.

The 5′-amino groups were coupled to either fluorescein-5-isothiocyanate (FITC) or tetramethylrhodamine isothiocyanate (TRITC). The coupling conditions, removal of excess reagents with spin-down gel-filtration, and the final purification by high-pressure liquid chromatography (HPLC) were made as described previously (21) with the modifications noted by Fenchel and Ramsing (13). The purity of the resulting probes was checked by analytical HPLC and by gel electrophoresis and was found to be more than 95% labeled oligonucleotides with the appropriate length. Stock solutions were dissolved in 10 mM NaCl–10 mM sodium cacodylate (pH 7.2) and stored at −20°C.

Hybridization. The hybridization solution was composed of 5× SSC, 10× Denhardt's solution, 0.5 mg of poly(A) per ml, 0.1% Triton X-100, 21% deionized formamide, and 5 ng of each fluorescent probe per μl. Many different combinations of probes were tried with mixtures of one probe labeled with FITC and another with TRITC. However, because of the strong inherent green fluorescence when samples were excited with blue light, we were unable to discriminate cells with the FITC-labeled probes (see below). Hybridization solution (60 μl) was applied to each slide, which was covered with a coverslip to prevent evaporation and placed in an airtight box containing a cloth soaked in the prehybridization solution.

The incubation took place at 37°C for 4 h. The slides were subsequently washed with 50 ml of 21% formamide in 5× SSC for 10 min at 37°C. Excess liquid was removed, and the slides were allowed to air dry before being mounted in Mowiol (Hoechst, Frankfurt, Germany).

Epifluorescence microscopy. The slides were examined with a Zeiss Axioplan epifluorescence microscope with three standard Zeiss filter sets: 01 (UV excitation, blue emission [for Hoechst 33258 and DAPI staining]); 10 (blue excitation, green emission [selectively for FITC]), and 15 (green excitation, red emission [for TRITC]). Besides the standard filter sets, two additional emission filters were used: (i) a narrow-bandpass filter, Corion SS 590 (585 to 595 nm), which was used together with the filter set 15 for selective observation of light emitted from rhodamine probes; and (ii) a short-pass filter, Balzars K2, that was used for selective observation of Hoechst 33258 and DAPI (i.e., blue and green fluorescence). A 10× ocular with counting grid and a 63× plan-NEOFLUAR oil immersion objective were used for cell counting. The pictures presented were taken with a 100× plan-NEOFLUAR oil immersion objective without additional magnification.

The microscope was equipped with a Peltier-cooled Photometrics slow-scan charge-coupled device (CCD) camera with a Metachrome II extended UV CCD chip (KAF 1400; 1,320 by 1,035 pixels, 500-kHz transfer rate, pixel size 6.8 by 6.8 μm). The camera was controlled by a Mac IIfx computer with a Photometrics CCD camera controller. Digital pictures were acquired as 12-bit images with the program NU 200 (Photometrics). The pictures were subsequently exported as 8-bit TIFF files, which were analyzed with the program NIH Image v. 1.47. This program is freely available from the anonymous FTP site: zippy.nimh.nih.gov on Internet. Manipulations consisted of sharpening, adding of pseudocolors, and combining and scaling the pictures for the transects shown in Fig. 4a and b.

RESULTS

Reference cells and hybridization conditions. The specificity of the hybridization reaction was verified with three mixtures of reference cells deposited next to each biofilm slice. The mixtures contained both positive and negative controls, the latter being cells with extremely high ribosomal content (*Saccharomyces cervisiae* and *E. coli*) or phylogenetically related cells (*Pseudomonas* spp.). The reference cell mixtures were used to optimize the hybridization conditions. A strong improvement in fluorescence signal, specificity, and reproducibility was achieved by adding deionized formamide to the hybridization solution. The optimum formamide concentration at a constant hybridization temperature of 37°C varied only slightly for the different probes, 20 to 24%, so a mean concentration of 21% was chosen. After the hybridization conditions had been optimized, all the probes stained all of the reference cells that they were designed to stain but none of the other reference cells. Representative staining of the different cell mixtures is shown in Fig. 1.

Inherent fluorescence. An eminent problem when working with fluorescent probes in a compact photosynthetic community is the intrinsic fluorescence from fluorescent pigments. The light emitted from different fluorophores, however, had different spectral compositions. When exciting a biofilm sample with green light and observing the emitted red fluorescence, the light emitted from rhodamine-labeled oligonucleotide probes was more yellow than the light emitted from inherent fluorophores such as chlorophyll *a*. It was thus possible to identify individual TRITC probe-stained cells in the biofilm. The labeled cells appear to the observer as small orange-yellow objects that are, however, difficult to photograph since most high-sensitivity films and CCD cameras exhibit high sensitivity far into the infrared. A way around this problem is to use an additional narrow-bandpass filter that allows only orange-yellow light in the range of 585 to 595 nm to pass through. This cuts off most of the intrinsic fluorescence, making the probe-labeled cells stand out more clearly. However, it also reduces the total light intensity to <1%, which necessitates the use of a highly sensitive camera such as the Peltier cooled slow-scan camera used in this study. We used a Corion SS 590 filter together with the ordinary TRITC filter set for selective observation of light emitted from rhodamine probes (42).

Unfortunately, we were not able to find a selective filter set to enhance the fluorescence of FITC-labeled cells. It was thus not possible in these samples to do a simultaneous staining with two probes of different specificities, i.e., a

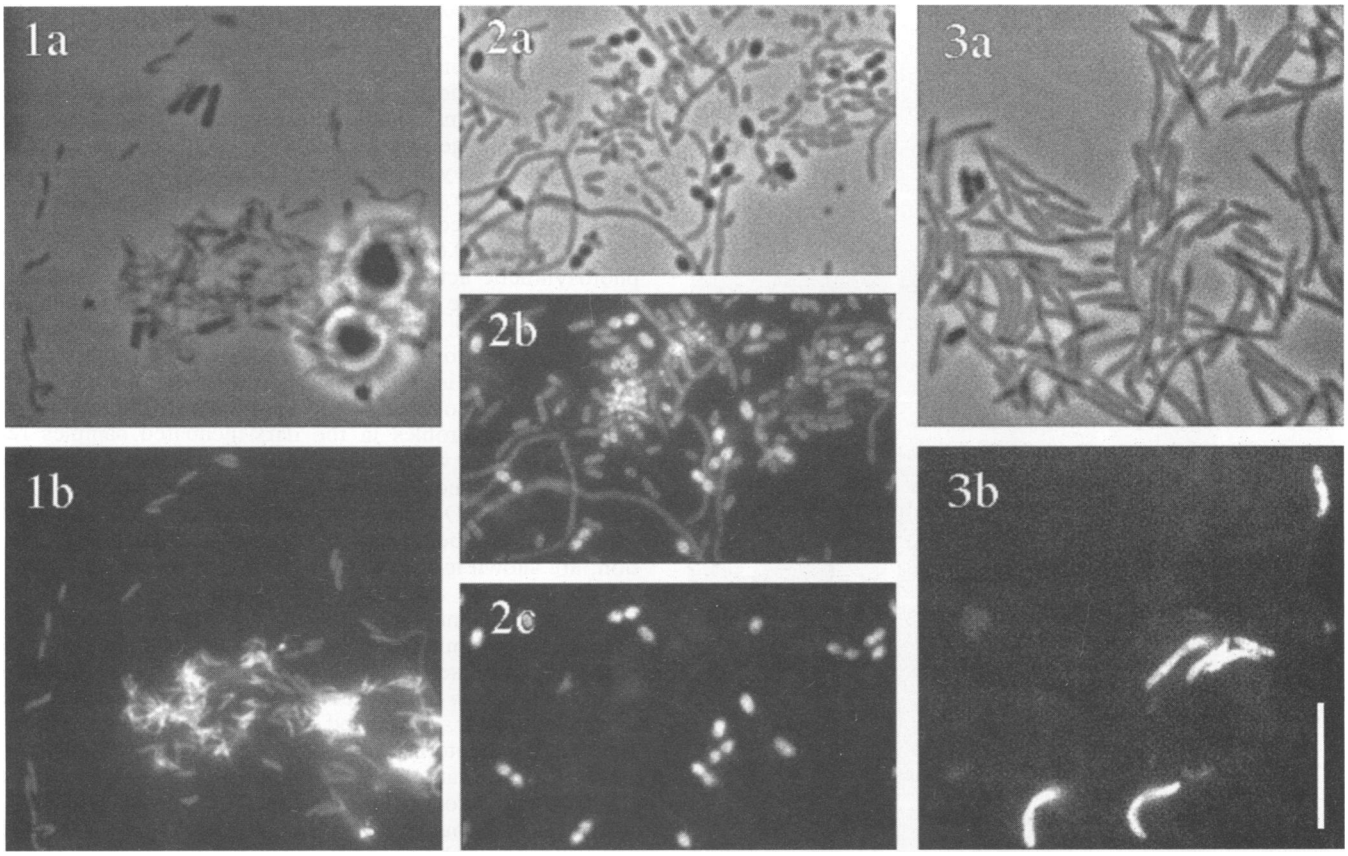

FIG. 1. Specificity of fluorescent oligonucleotide probes checked by staining of three different mixtures of cell cultures. For comparison, phase-contrast micrographs of the same microscopic fields show all cell types present (1a, 2a, and 3a). 1a, *E. coli* (thick rods), *S. cervisiae* (large highly refractory cells), and *Desulfovibrio vulgaris* (small thin slightly vibrioid); 1b, bacteria in panel 1a stained with a rhodamine-labeled SRB probe; 2a, *P. cepacia* (long filaments), *P. aeroginosa* (small short rods, low refractance), and *Desulfobulbus propionicus* (ellipsoid, strong refractance, often doublets); 2b, bacteria in panel 2a stained with a fluorescein-labeled eubacterial probe; 2c, bacteria in panel 2a stained with a rhodamine-labeled SRB probe; 3a, *P. fluorescens* (long slender rods), *Desulfovibrio gigas* (large vibrios similar to *P. fluorescens*), *Desulfobacter curvatus* (short refractory ellipsoids); 3b, bacteria in panel 3a stained with a rhodamine-labeled SRB probe. The white bar in frame 3b corresponds to 10 μm and applies to all images.

combined stain with the SRB probe and the general eubacterial probe, one being FITC labeled and the other being labeled with TRITC.

In situ detection of SRB. Figure 2 shows representative pictures of the dark-incubated biofilm stained with the rhodamine-labeled SRB probe. The first panel (Fig. 2.1) is a composite image made of 13 phase-contrast images on a vertical transect down through the biofilm. The digital images were combined and scaled (program NIH image v. 1.44) to give an impression of the overall structure of the biofilm. The second panel (Fig. 2.2) is a similar composite image of the red fluorescence along the same transect by using a standard filter set for rhodamine (Zeiss filter set 15). The third set of panels (Fig. 2.3a to 2.3g) are close-up views with the same filter set at various depths. The fourth set of panels (Fig. 2.4a to 2.4g) shows the same close-up views with both the standard filter set and the selective narrow-bandpass filter centered around 590 nm. By comparing the two sets of panels (Fig. 2.3a to 2.3g and 2.4a to 2.4g), cells that have been labeled by the SRB probe become apparent. The positive cells are clearly visible on the images taken with the selective filter (Fig. 2.4a to 2.4g) and less so on the ones taken with the general filters (Fig. 2.3a to 2.3g). The panels are ordered according to the depth at which they were acquired.

SRB probe-stained cells were found at all depths except for the uppermost part of the *Oscillatoria* layer. The first set of close-up figures (Fig. 2.3a and 2.4a) were taken at a depth of about 0.4 mm. The general SRB probe stained cells of all morphologies and sizes including cocci, rods, vibrios, and some unusual "filamentous" cells. The filamentous cells appeared to develop inside decaying cyanobacteria and were thus found only in a narrow zone at the bottom of the *Oscillatoria* layer (see below). Potential precursors to the filaments were short rods adhering to (or living inside?) apparently intact *Oscillatoria* cells. These cells were some of the uppermost SRB probe-positive cells. Slightly deeper, we found long chains inside decaying *Oscillatoria* cells (Fig. 2.3b and 2.4b). The characteristic chains appeared to fuse into long filaments when the cyanobacteria were almost completely degraded (Fig. 2.3c and 2.4c). The decay of the *Oscillatoria* cells was inferred from a markedly reduced pigment content and an irregular appearance. A striking finding was the irregular distribution of positive SRB cells. It ranged from randomly distributed individual cells (Fig. 2.3d and 2.4d) over loose assemblies of cells (Fig. 2.3e and 2.4e)

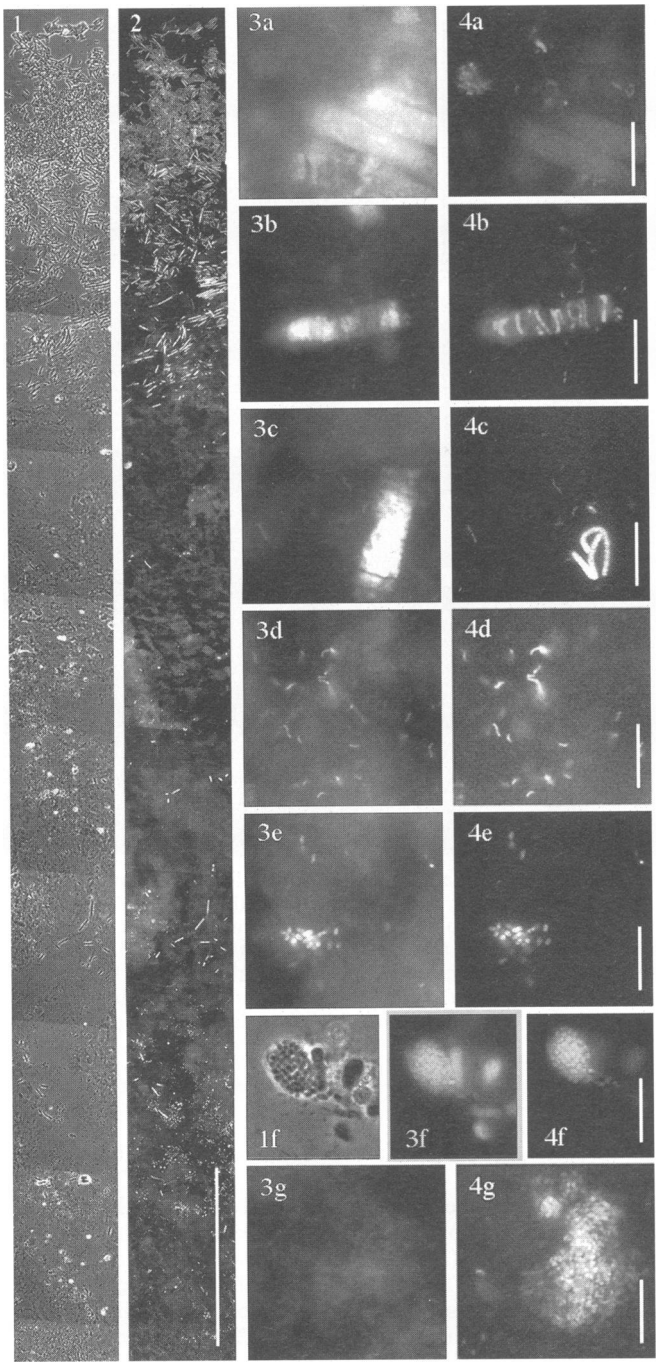

FIG. 2. Biofilm slice stained with rhodamine-labeled SRB probe. 1, Transect combined from 13 phase-contrast images taken down through the biofilm. 2, The same transect showing intrinsic red fluorescence. The white bar at the bottom right corner corresponds to 500 μm and applies to both transects. 3, close-up of the red fluorescence in frame 2 at different depths, using ordinary rhodamine filters. 4, The same frames observed through a narrow-bandpass filter centred at 590 nm. All bars in the small frames of panel 4 correspond to 10 μm. Panels a to g are defined in the text.

to densely packed clusters. The latter could contain many thousands of cells (Fig. 2.3g and 2.4g) or just tens to hundreds (Fig. 2.3f and 2.4f). All cells in a particular cluster were of the same size and morphology, but different clusters were found with very different sizes and different morphologies (e.g., small vibrios or large cocci); however, short rods or cocci predominated.

Chemical gradients. The chemical gradients within the biofilm were examined at high spatial resolution with microelectrodes. Oxygen profiles measured in the illuminated samples all displayed a distinct peak just below the surface, indicative of high photosynthetic activity. The oxygen penetration decreased gradually during the 48-h incubation, from 1.2 to ca. 0.6–0.8 mm. Representative profiles of O_2, photosynthetic activity, pH, and ΣH_2S, measured just before freezing, are shown in Fig. 3a. The peak in oxygen concentration just below the surface was accompanied by a peak in pH due to CO_2 fixation during photosynthesis. The subsequent drop in pH below the photic zone is ascribed to the high respiration rate within the biofilm.

The oxygen profiles in the dark-incubated samples remained constant, with steep oxygen gradients at the biofilm-water interface and depletion of oxygen within the upper 0.2 mm. Profiles of O_2, pH, and ΣH_2S measured at the end of incubation, just before rapid freezing, sectioning, and fixation, are shown in Fig. 4a.

The structure and stratification of the light-incubated biofilm differed markedly from those of the dark-incubated sample. The illuminated biofilm was thinner (3.4 versus 4.9 mm) with a sparser surface population of motile cyanobacteria (*Oscillatoria* sp.), since these had spread out over the surrounding agar. A detailed chemical, optical, and microstructural characterization of the biofilm is presented elsewhere (32); in that study, net metabolic rates were derived from measured concentration profiles.

Vertical distribution of SRB. To quantify the SRB and ascertain the reliability of the staining, we performed a blind experiment. Three slices of each sample (light or dark incubated) were stained with the rhodamine *Desulfobacter* probe, three were stained with the rhodamine SRB probe, and three were stained with the rhodamine control probe. The 18 slides were randomly mixed, and the number of positive cells along two vertical transects on each slide was counted, without knowledge of the probe that had been used to stain the particular slide. The transects were made by counting the cells within a counting grid, advancing the view one frame, and repeating the counts. Altogether, more than 400 microscopic fields were examined, giving a total of more than 10,000 positive cells. After all the transects were counted, the code was revealed, and the staining of the reference cell mixtures on each slide was checked against the expected results. All mixtures were found to be stained as expected. The counts were recalculated to absolute cell densities from the area of the counting grid and the visible depth range. The latter was estimated within the biofilm slice to ca. 5 μm, beneath which individual positive cells were no longer discernible from the background fluorescence in the biofilm matrix.

Figure 3 presents the depth distribution of positive cells for the three different probes in the illuminated sample, relative to gradients of O_2, ΣH_2S, pH, and photosynthesis. Figure 4 presents similar data for the biofilm sample incubated in the dark. In both light and dark experiments, cell counts with the negative control probe were negligible compared with counts with the SRB probe. The results indicate that the vast majority of the SRB-positive cells are true positives because they have bound the TRITC-labeled SRB-probe. Whether the probe-binding cells are truly SRB is, however, a different matter. We have used stringent hybridization conditions and have counted only strongly

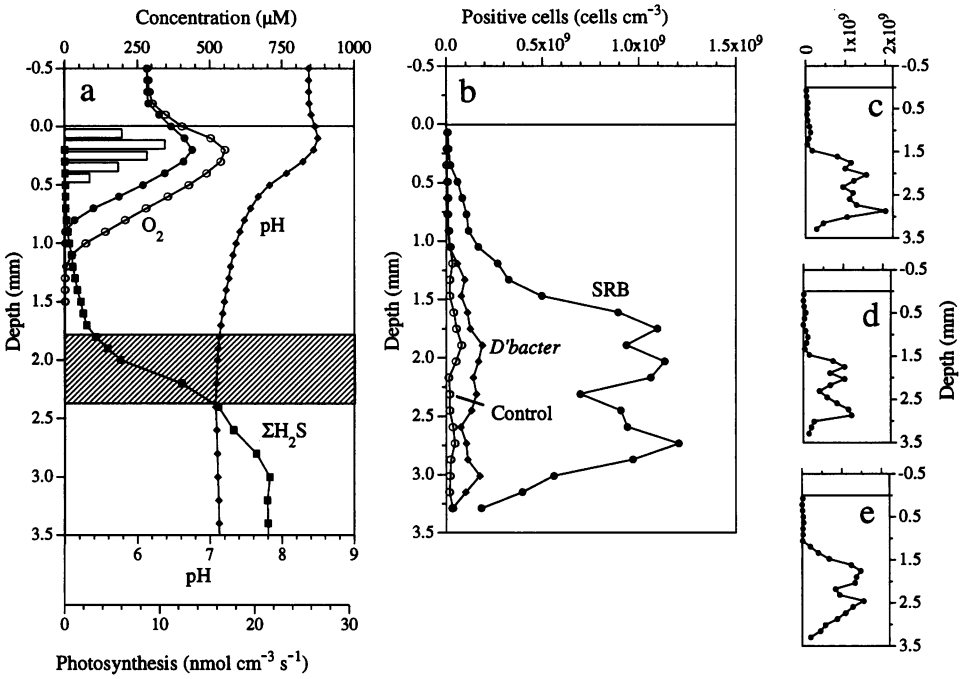

FIG. 3. Chemical parameters and cell densities of SRB in the light-incubated biofilm sample. (a) Microprofiles of oxygen concentration before (○) and after (●) 48 h of light incubation, total sulfide concentration (■), pH (◆), and rate of photosynthesis (bars). The hatched area indicates a dark band of FeS, which was probably responsible for the change in the ΣH_2S gradient in this region. (b) Average cell density in the light-incubated biofilm estimates from cell counts with the SRB probe (●), the *Desulfobacter* probe (◆), and the negative control probe (○). (c to e) Examples of SRB cell densities estimated from single transects, to show the variation between individual transects.

stained positives. Furthermore, the low counts with the negative control probe as well as the discriminative staining of the accompanying reference cells also substantiated a high specificity in the biofilm samples. We thus believe that the SRB probe-stained cells are indeed sulfate reducers.

The distribution of SRB probe-positive cells in the upper part of the biofilm of the light-incubated sample was notably different from that in the dark-incubated sample. In the illuminated sample we found only a few positive cells at all depths down to about 1.1 mm. In the dark-incubated biofilm

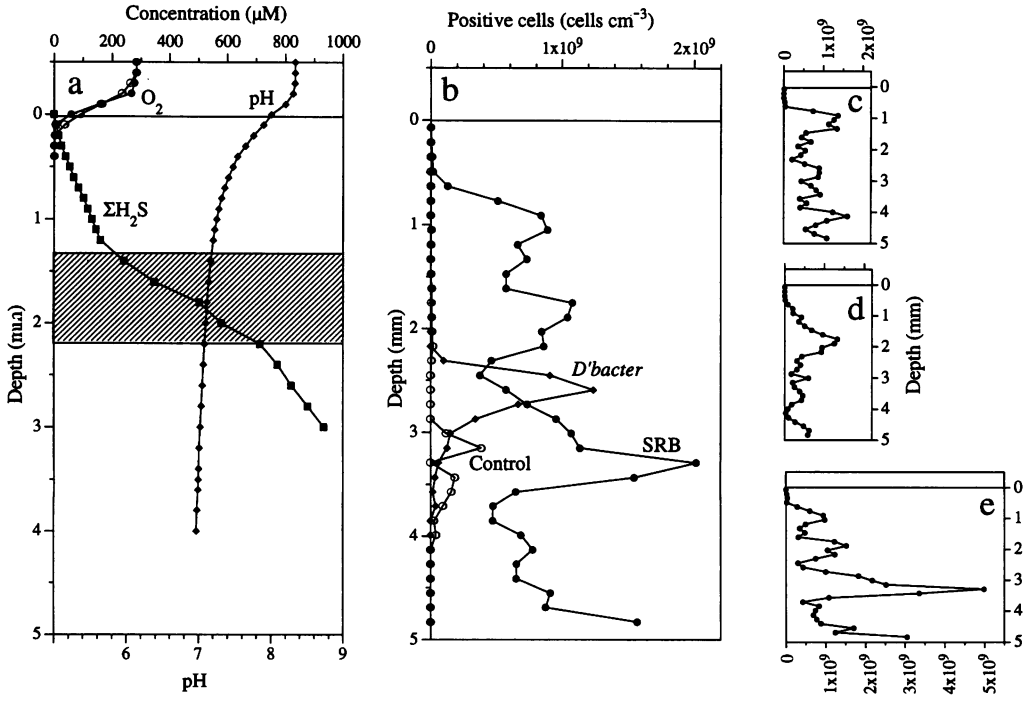

FIG. 4. Dark-incubated biofilm sample. Panels and symbols are as in Fig. 3.

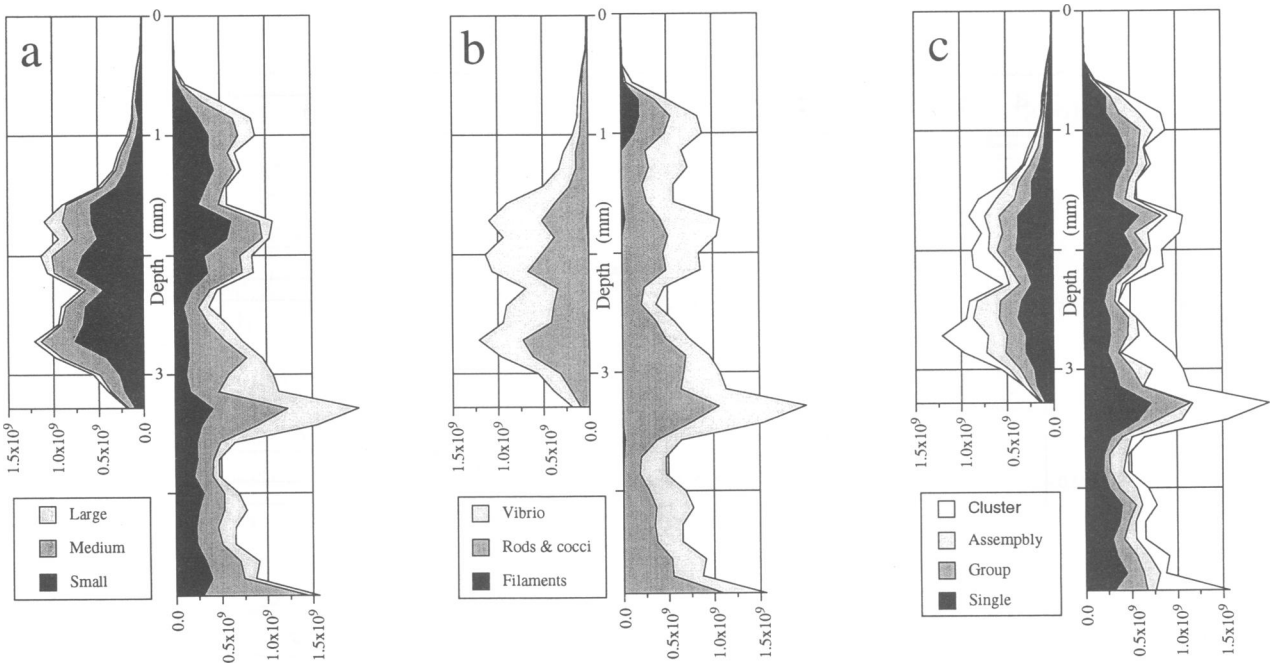

FIG. 5. Distribution of SRB cell size, morphology, and degree of clustering within the biofilm. Profiles to the left in each panel show the light-incubated sample, and those to the right show the dark-incubated sample. At any depth, the outermost curve corresponds to the total number of SRB, which are then divided into different categories. The number of cells belonging to a particular category is indicated by the areas with different shades. (a) The total population divided into size classes. (b) The total population divided into classes pertaining to morphology. (c) The total population divided into classes pertaining to the degree of clustering (see text).

there were large numbers of SRB from 0.5 to 0.6 mm below the surface. The difference was found in virtually all transects and is ascribed to the different oxygen penetrations in the two samples. The SRB thus appear to be excluded from the oxic zone.

We found no significant difference between the average cell counts in the anoxic part of the dark-incubated and light-incubated samples, ca. 1.0×10^9 cells per cm^3. Previous counts from marine sediments were 1 to 6 orders of magnitude lower (19, 26, 43, 44). This is, to our knowledge, the highest reported density of SRB in a natural environment. Assuming a mean cell volume of 1 μm^3, this corresponds to 1‰ of the total volume being biovolume of SRB. In both cases the SRB probe-stained cells were distributed throughout the film below the oxic zone, with no notable peak abundance at any depth. (The small peaks on the average curves were due to clusters in a single transect [see below].)

Cells positive for the *Desulfobacter* probe. Only a few positive cells were found by the *Desulfobacter* probe, and their fluorescence intensity was low, partly because of their small size. The counts obtained in the illuminated sample were about twice the counts of the negative control, whereas for the dark-incubated sample they were even lower. Bacteria of this genus thus appear to be a minor component of the SRB population in the biofilm. This is not so surprising since the genus is found mostly in marine environments (48). The prominent peak of positive cells in the dark-incubated sample at about 2.5-mm depth was due to a large cluster in one of the transects of slightly fluorescent short rods, which could possibly be false positives.

Cell size, morphology, and clustering. As the positive cells were counted along the transects, their size, morphology, and degree of clustering were noted and expressed as a percentage of the cell count in the particular frame. Three size classes were noted: small (less than 1 μm long), medium (1 to 2.5 μm long), and large (more than 2.5 μm long). The cell size distribution in light and dark is shown in Fig. 5a. The bacteria were larger on average in the dark-incubated sample, but the size composition was relatively constant at all depths.

Cells were also categorized into three morphology classes: rods plus cocci, vibrios, and filaments. A constant 1:1 ratio of rods plus cocci to vibrios was found in both incubations at all depths (Fig. 5b). Since many vibrios were probably misplaced into the rods-plus-cocci category because of their vertical orientation, they were probably the dominant morphotype in the sample. The long filamentous cells mentioned above were found in a relatively narrow region, just beneath the oxic layer (Fig. 5b). They were much more frequent in the dark-incubated sample in accordance with the increased occurrence of decaying *Oscillatoria* cells, possibly dying because of light deprivation.

Positive cells were assigned to one of four distribution categories: single, loosely grouped, part of an assembly, or part of a dense cluster of cells. Figure 5c shows the relative predominance of each of the four categories. Randomly distributed and loosely grouped cells were found in rather constant numbers at all depths, whereas assemblies and especially clusters caused peaks in the average cell distributions. These clusters were found at different depths in different transects and could be found at all depths. They were not more frequent in or near the oxic zone, nor were they larger in that zone. There was thus no support in the present data for the occurrence of SRB mostly clustered in anoxic microenvironments within oxic or oxidized zones.

DISCUSSION

Rate calculations. Rates of both photosynthetic and heterotrophic metabolism are very high in the trickling-filter biofilm. Since the cells in this type of biofilm are growing and dividing rapidly, they are assumed to have a high ribosome content per cell and are thus well suited for the use of oligonucleotide probes that bind to 16S rRNA (10). It is possible that the counted cells represent only a small fraction of the total population of SRB. This can be evaluated by comparing calculated rates of sulfate reduction and observed cell densities with sulfate reduction per cell in pure cultures.

Sulfate reduction rates in these (32) and similar (25) biofilms were calculated by modeling sulfide distribution. For dark-incubated samples with 0.5 to 0.8 mM SO_4^{2-} in the overlying water, a constant rate of about 0.5 μmol of S cm^{-3} h^{-1} at all depths below 0.7 mm was observed (25, 32). This agrees well with the uniform average distribution of SRB in Fig. 3b and 4b.

Maximum sulfate reduction rates, V_{max}, in the range of 800 to 2,600 μmol of S g of dry cell $mass^{-1}$ h^{-1} have been reported for pure cultures of different *Desulfovibrio* spp. (48). Assuming a cell volume of 1 to 10 μm^3 (48) with 5% dry weight and using the observed sulfate reduction rate and V_{max}, one would expect SRB population densities in the range of 1×10^8 to 8×10^8 cells cm^{-3}. Even though the sulfate concentration in this experiment exceeded reported K_m values (5 to 216 μM) (48), other substrates are expected to be limiting (25), so that the actual sulfate reduction rate per cell is lower than the V_{max} reported previously (48). The number of SRB required to account for the measured sulfate reduction rate in the biofilm must therefore be greater than 1×10^8 to 8×10^8 cells cm^{-3}. The predicted numbers agree well with the observed numbers of ca. 10^9 cells cm^{-3}. The agreement indicates that at least a significant fraction of all SRB present were counted. It is anticipated that not all SRB were counted as positive cells because of the selective hybridization conditions that were used. We were likely to miss phylogenetically deviating organisms as well as dormant or starved cells with low ribosomal content.

Evaluation of the hybridization conditions. The hybridization conditions that we have used in this study deviate from those used in previous studies (4, 6). The main difference is the addition of formamide to the hybridization and wash solutions and a resulting reduction of the temperature used in these steps. The dissociation temperature of oligonucleotides of between 10 and 50 bp can be calculated from the formula of Lathe (27), corrected for the influence of formamide (28, 38):

$$T_d = 81.5 + 16.6 \log_{10} M + 0.41[\%(G+C)] - (820/n) - 0.7(\%f) \quad (1)$$

where T_d is the dissociation temperature in degrees Celsius, M is the molar cation concentration, %(G+C) is the percentage of guanine plus cytosine bases in the oligonucleotide, n is the length (in base pairs) of the oligonucleotide, and f is the formamide concentration. With this formula to compare hybridization conditions, our hybridization temperature is closer to the dissociation temperature than that used in previous studies (4, 6) and the hybridization conditions are thus slightly more stringent (i.e., more selective). However, the formula above is in many cases not adequate to predict optimal hybridization conditions; i.e., it does not include effects of probe and target concentrations or the enthalpy of duplex formation. A more rigorous treatment of the thermodynamics of duplex formation obtained by using the simplest possible model, a concerted two-state model, gives (31, 33)

$$\frac{1}{T_m} = \frac{\Delta S}{\Delta H_{vH}} - \frac{R}{\Delta H_{vH}} \ln\left(c_p - \frac{c_t}{2}\right) \quad (2)$$

where T_m is the temperature at which half of the target rRNA has bound an oligonucleotide probe, which is equivalent to T_d; ΔS is the enthalpy of duplex formation, ΔH_{vH} is van't Hoff's enthalpy of transition (which for short oligonucleotides can be estimated as roughly 25 kJ mol^{-1} K^{-1} per bp [33]), R is the gas constant, and c_p and c_t are the probe and the target concentrations, respectively. The concentration dependence of T_m can explain a common discrepancy between the hybridization conditions that are used with membrane-bound targets (usually at or above T_d as predicted by equation 1 [12, 39, 41]) and the ones used in in situ hybridization experiments (usually at least 10°C below T_d [4–6, 13, 17, 41]), even with the same set of probes, by assuming vastly different probe and target concentrations in the two cases.

The relationship between melting temperature and probe-target concentration points to a basic problem with many of the current protocols for in situ hybridization. These protocols include several washing steps in which the probe concentration is virtually unknown and consequently the melting temperature is often irreproducibly altered. Therefore, it is often very difficult to compare different protocols or even to repeat experiments performed in other laboratories, let alone to predict the stringency of particular hybridization conditions. Empirical formulas such as equation 1 require that the all parameters not included in the formula be kept constant if they are to retain predictive ability.

The best test which we have used to check the specificity of the hybridization conditions is the concurrent reproducible and discriminative staining of reference cells. It should be noted that the general SRB probe only vaguely stained the *Desulfobacter curvatus* reference cells (e.g., the two dense oval rods near the left edge of Fig. 3.3a and 3.3b). This was not surprising since the target sequence in *Desulfobacter* spp. (and in *Desulfosarcina* spp.) has one mismatch with the general SRB probe (4). The inability to stain these organisms therefore suggests that we have achieved a high specificity in this study.

Conclusion. We believe that oligonucleotide probes can now be used to determine the spatial distribution of SRB in complex natural environments, provided suitable reference organisms are included in the experiment (as both negative and positive controls). The hybridization conditions used in this study were intended to be restrictive, to avoid the possibility that non-SRB would be counted as positive. The counts consequently represent only the fast-growing part of the SRB population. However, when the total counts are compared with measured sulfate reduction rates, a significant proportion of the total population appears to have been identified. Although we did not find significant numbers of SRB in the upper, oxic layers, they could still be present if (i) they belong to a different yet uncharacterized phylogenetic group of sulfate reducers, (ii) they are mainly dormant or slowly metabolizing cells, or (iii) they have, as part of their adaptation to the oxic environment, developed a particularly rigid cell wall, which is impermeable to our probes. A prominent finding of this study was the heterogeneity of the cell distribution. Most of the cells were present in dense clusters or assemblies, reflecting the overall heterogeneity of the material but at the same time discouraging cell counting.

New techniques to overcome these problems by using extensive computer analysis of acquired images are currently being developed in our laboratory. These include digital deconvolution with appropriate pointspread functions to obtain haze-free confocal images (1, 2) and subsequent particle identification by watershed thresholding (20) (in which the image is subdivided into smaller areas and to which individual thresholds are applied). The present approach of using microelectrodes together with specific oligonucleotide probes proved fruitful in that it was possible to relate the distribution of genetically defined bacteria to their chemical microenvironment at a spatial resolution of 100 μm. We foresee interesting prospects in the combination of these two high-resolution techniques. The techniques have general applicability to studies of other bacterial processes, e.g., the use probes for denitrifying bacteria together with microelectrodes for nitrous oxide (29) or nitrate (9).

ACKNOWLEDGMENTS

These studies were supported by the Max Planck Society, Germany.

We are indebted to Thomas M. Jovin, Max Planck Institute for Biophysical Chemistry, Göttingen, Germany, for generously providing equipment and materials and to David A. Stahl and Rudolf Amann for discussions. We also thank Karsten Rippe and Gudrun Heim for helpful assistance during probe preparation, as well as Åse Lyhr for cutting biofilm samples on a cryomicrotome.

REFERENCES

1. **Agard, D.** 1984. Optical sectioning microscopy: cellular architecture in three dimensions. Annu. Rev. Biophys. Bioeng. **13:**191–219.
2. **Agard, D., H. Yasushi, and J. Sedat.** 1989. Three-dimensional microscopy: image processing for high resolution subcellular imaging, p. 24–30. *In* J. Wampler (ed.), New methods in microscopy and low light imaging.
3. **Amann, R., N. Springer, W. Ludwig, H.-D. Görtz, and K.-H. Schleifer.** 1991. Identification *in situ* and phylogeny of uncultured bacterial endosymbionts. Nature (London) **351:**161–164.
4. **Amann, R. I., B. J. Binder, R. J. Olson, S. W. Chrisholm, R. Devereux, and D. A. Stahl.** 1990. Combination of 16S rRNA-targeted oligonucleotide probes with flow cytometry for analyzing mixed microbial populations. Appl. Environ. Microbiol. **56:**1919–1925.
5. **Amann, R. I., L. Krumholz, and D. A. Stahl.** 1990. Fluorescent-oligonucleotide probing of whole cells for determinative, phylogenetic, and environmental studies in microbiology. J. Bacteriol. **172:**762–770.
6. **Amann, R. I., J. Stromley, R. Devereux, R. Key, and D. A. Stahl.** 1992. Molecular and microscopic identification of sulfate-reducing bacteria in multispecies biofilms. Appl. Environ. Microbiol. **58:**614–623.
7. **Canfield, D. E., and D. J. Des Marais.** 1991. Aerobic sulfate reduction in microbial mats. Science **251:**1471–1473.
8. **Dalsgaard, T., and N. P. Revsbech.** 1992. Regulating factors of denitrification in trickling filter biofilms as measured with the oxygen/nitrous oxide microsensor. FEMS Microbiol. Ecol. **101:** 151–164.
9. **DeBeer, D., and J. P. R. A. Sweerts.** 1989. Measurement of nitrate gradients with an ion selective microelectrode. Anal. Chim. Acta **219:**351–356.
10. **DeLong, E. F., G. S. Wickham, and N. R. Pace.** 1989. Phylogenetic stains: ribosomal RNA-based probes for the identification of single cells. Science **243:**1360–1363.
11. **Devereux, R., M. Delaney, F. Widdel, and D. A. Stahl.** 1989. Natural relationships among sulfate-reducing eubacteria. J. Bacteriol. **171:**6689–6695.
12. **Devereux, R., M. D. Kane, J. Winfrey, and D. A. Stahl.** 1992. Genus-specific and group-specific hybridization probes for determinative and environmental studies of sulfate-reducing bacteria. Syst. Appl. Microbiol. **15:**601–609.
13. **Fenchel, T., and N. B. Ramsing.** 1992. Identification of sulfate-reducing ectosymbiotic bacteria from anaerobic ciliates using 16S rRNA binding oligonucleotide probes. Arch. Microbiol. **158:**394–397.
14. **Fründ, C., and Y. Cohen.** 1992. Diurnal cycles of sulfate reduction under oxic conditions in cyanobacterial mats. Appl. Environ. Microbiol. **58:**70–77.
15. **Giovannoni, S. J., E. F. DeLong, G. J. Olsen, and N. R. Pace.** 1988. Phylogenetic group-specific oligodeoxynucleotide probes for identification of single microbial cells. J. Bacteriol. **170:**720–726.
16. **Glud, R. N., N. B. Ramsing, and N. P. Revsbech.** 1992. Photosynthesis and photosynthesis-coupled respiration in natural biofilms measured by use of oxygen microsensors. J. Phycol. **28:**51–60.
17. **Hicks, R. E., R. I. Amann, and D. A. Stahl.** 1992. Dual staining of natural bacterioplankton with 4′,6-diamidino-2-phenylindole and fluorescent oligonucleotide probes targeting kingdom-level 16S rRNA sequences. Appl. Environ. Microbiol. **58:**2158–2163.
18. **Jørgensen, B. B.** 1977. Bacterial sulfate reduction within reduced microniches of oxidized marine sediments. Mar. Biol. **41:**7–17.
19. **Jørgensen, B. B., and F. Bak.** 1991. Pathways and microbiology of thiosulfate transformations and sulfate reduction in a marine sediment (Kattegat, Denmark). Appl. Environ. Microbiol. **57:** 847–856.
20. **Jovin, T. M., and D. J. Arndt-Jovin.** 1991. Digital imaging microscopy: the marriage of spectroscopy and the solid-state CCD camera. SPIE Proceedings, Georgetown, Grand Cayman Island.
21. **Jovin, T. M., K. Rippe, N. B. Ramsing, R. Klement, W. Elhorst, and M. Voijtiskova.** 1990. Parallel stranded DNA, p. 155–174. *In* R. H. Sarma and M. H. Sarma (ed.), Structure & methods, DNA & RNA. Adenine Press, Schenectady, N.Y.
22. **Jurtshuk, R. J., M. Blick, J. Bresser, G. E. Fox, and P. Jurtshuk.** 1992. Rapid in situ hybridization technique using 16S rRNA segments for detecting and differentiating the closely related gram-positive organisms *Bacillus polymyxa* and *Bacillus macerans*. Appl. Environ. Microbiol. **58:**2571–2578.
23. **Kuenen, J. G., B. B. Jørgensen, and N. P. Revsbech.** 1986. Oxygen microprofiles of trickling filter biofilms. Water Res. **20:**1589–1598.
24. **Kühl, M.** 1992. Photosynthesis, O_2 respiration and sulfur cycling in a cyanobacterial biofilm. Proceedings of the 6th International Symposium on Microbial Ecology, Barcelona.
25. **Kühl, M., and B. B. Jørgensen.** 1992. Microsensor measurements of sulfate reduction and sulfide oxidation in compact microbial communities of aerobic biofilms. Appl. Environ. Microbiol. **58:**1164–1174.
26. **Laanbroek, H. J., and N. Pfennig.** 1981. Oxidation of short-chain fatty acids by sulfate-reducing bacteria in freshwater and in marine sediments. Arch. Microbiol. **128:**330–335.
27. **Lathe, R.** 1985. Synthetic oligonucleotide probes deduced from amino acid sequences data. Theoretical and practical considerations. J. Mol. Biol. **183:**1–12.
28. **McConaughy, B. L., C. D. Laird, and B. J. McCarthy.** 1969. Nucleic acid reassociation in formamide. Biochemistry **8:**3289–3295.
29. **Nielsen, L. P., P. B. Christensen, N. P. Revsbech, and J. Sørensen.** 1990. Denitrification and oxygen respiration in biofilms studied with a microsensor for nitrous oxide and oxygen. Microb. Ecol. **19:**63–72.
30. **Poulsen, L. K., G. Ballard, and D. A. Stahl.** Use of rRNA fluorescence in situ hybridisation for measuring the activity of single cells in early and established biofilms. Submitted for publication.
31. **Ramsing, N. B., and T. M. Jovin.** 1988. Parallel stranded duplex DNA. Nucleic Acids Res. **16:**6659–6676.
32. **Ramsing, N. B., M. Kühl, and B. B. Jørgensen.** Unpublished data.

33. **Ramsing, N. B., K. Rippe, and T. M. Jovin.** 1989. Helix-coil transition of parallel-stranded DNA. Thermodynamics of hairpin and linear duplex oligonucleotides. Biochemistry **28:**9528–9535.
34. **Rehnstam, A.-S., A. Norqvist, H. Wolf-Watz, and Å. Hagström.** 1989. Identification of *Vibrio anguillarum* in fish by using partial 16S rRNA and a specific 16S rRNA oligonucleotide probe. Appl. Environ. Microbiol. **55:**1907–1910.
35. **Revsbech, N. P.** 1989. An oxygen microelectrode with a guard cathode. Limnol. Oceanogr. **34:**474–478.
36. **Revsbech, N. P., and B. B. Jørgensen.** 1983. Photosynthesis of benthic microflora measured with high spatial resolution by the oxygen microprofile method: capabilities and limitations of the method. Limnol. Oceanogr. **28:**749–756.
37. **Spring, S., R. Amann, W. Ludwig, K.-H. Schleifer, and N. Petersen.** 1992. Phylogenetic diversity and identification of nonculturable magnetotactic bacteria. Syst. Appl. Microbiol. **14:** 116–122.
38. **Stahl, D. A., and R. Amann.** 1991. Development and application of nucleic acid probes, p. 205–248. *In* E. Stackebrandt and M. Goodfellow (ed.), Nucleic acid techniques in bacterial systematics. John Wiley & Sons Inc., New York.
39. **Stahl, D. A., B. Flesher, H. R. Mansfield, and L. Montgomery.** 1988. Use of phylogenetically based hybridization probes for studies of ruminal microbial ecology. Appl. Environ. Microbiol. **54:**1079–1084.
40. **Stahl, D. A., and M. D. Kane.** 1992. Methods of microbial identification, tracking and monitoring of function. Curr. Opin. Biotechnol. **3:**244–252.
41. **Tsien, H. C., B. J. Bratina, K. Tsuji, and R. S. Hanson.** 1990. Use of oligonucleotide signature probes for identification of physiological groups of methylotrophic bacteria. Appl. Environ. Microbiol. **56:**2858–2865.
42. **Viles, C. L., and M. E. Sieracki.** 1992. Measurement of marine picoplankton cell size by using a cooled, charge-coupled device camera with image-analyzed fluorescence microscopy. Appl. Environ. Microbiol. **58:**584–592.
43. **Visscher, P. T., R. A. Prins, and H. von Gemerden.** 1992. Rates of sulfate reduction and thiosulfate consumption in a marine microbial mat. FEMS Microbiol. Ecol. **86:**283–294.
44. **Visscher, P. T., and H. von Gemerden.** 1991. Production and consumption of dimethylsulfoniopropionate in marine microbial mats. Appl. Environ. Microbiol. **57:**3237–3242.
45. **Wagner, M., R. Amann, H. Lemmer, and K.-H. Schleifer.** 1993. Probing activated sludge with oligonucleotides specific for proteobacteria: inadequacy of culture-dependent methods for describing microbial community structure. Appl. Environ. Microbiol. **59:**1520–1525.
46. **Ward, D. M., M. M. Bateson, R. Weller, and A. L. Ruff-Roberts.** 1992. Ribosomal RNA analysis of microorganisms as they occur in nature, p. 219–286. *In* K. C. Marshall (ed.), Advances in microbial ecology. Plenum Press, New York.
47. **Ward, D. M., R. Weller, and M. M. Bateson.** 1990. 16S rRNA sequences reveal numerous uncultivated microorganisms in a natural environment. Nature (London) **345:**63–65.
48. **Widdel, F.** 1988. Microbiology and ecology of sulfate- and sulfur-reducing bacteria. John Wiley & Sons, Inc., New York.
49. **Zarda, B., R. Amann, G. Wallner, and K.-H. Schleifer.** 1991. Identification of single bacterial cell using digoxigenin-labelled, rRNA-targeted oligonucleotides. J. Gen. Microbiol. **137:**2823–2830.